Desalination and Water Treatment
www.deswater.com
doi: 10.5004/dwt.2022.29068

279 (2022) 55–60
December

Synthesis, morphological and optical characterization of di-chromium three oxide nanoparticles

Hamza Kellou[a,b,*], Salem Boudinar[a], Abdelhafid Souici[b], Nassima Benbrahim[a]

[a]*Laboratoire de Physique et Chimie des Matériaux (LPCM), Université Mouloud MAMMERI de Tizi-Ouzou, BP 17, RP Tizi-Ouzou 15000, Algeria, Tel. +213540604059/+213556848909; email: hamza.kellou@ummto.dz (H. Kellou)*
[b]*Laboratoire de Physico-chimie des Matériaux et Catalyse (LPCMC), Université Abderrahmane Mira de Bejaïa, CP 06000, Bejaïa, Algeria*

Received 7 June 2022; Accepted 28 September 2022

ABSTRACT

In this study, chromium three oxide (Cr_2O_3) nanoparticles (NPs) were synthesized by a chemical method, using ($NaBH_4$) as a reducing agent at various concentrations. The obtained Cr_2O_3 NPs were characterized by scanning electron microscopy (SEM), UV-Vis and nitrogen adsorption–desorption measurements. The SEM analysis of the nanopowders, showed the formation of nanometer size particles. Fourier-transform infrared spectroscopy confirmed the Cr–O and Cr=O bands by their characteristic peaks. The values of the specific surface area of mesoporous powder changed according to the $NaBH_4$ concentration. UV-Vis spectrum for Cr_2O_3 NPs revealed two strong bands (in solution) and for the solid UV-Vis three peaks were seen. Finally, as an application, the effect of Cr_2O_3 nanoparticles (NPs) was monitored on 2-aminophenol dissolved in water under UV lamp irradiation (210 nm).

Keywords: Cr_2O_3 nanoparticles; Chemical synthesis; Specific surface area; Optical properties; 2-aminophenol

1. Introduction

Chromium is widely abundant on earth and can be found in various places such as in rocks, soil, animals, and plants. The current study assessed two oxidation states, trivalent chromium Cr^{3+} and hexavalent chromium Cr^{6+}. The very different physiological effects between Cr^{3+} and Cr^{6+}, have been investigated by a number of researchers. It was discovered that Cr^{3+} is an oligo-element. This means that a trace amount of this material is essential for the proper functioning of living organisms. On the other hand, Cr^{6+} is extremely toxic. Madrakian et al. [1] studied the presence of Cr^{6+} in tap water. Jamali et al. [2] assessed the potential accumulation of heavy metals (between them Cr) in vegetables grown in land treated for a long time with a mixture of wastewater and sewage sludge (SIDWS). They attributed the high percentage of Cd and Cr in SIDWS to waste effluent from small industries (tanneries and batteries) situated in domestic areas. Pouzar et al. [3] developed a procedure for analysis of chromium in a dyed wool fabric using a commercially available spectrometer. Salnikow and Zhitkovich [4] highlighted the differences between Cr^{6+} and Cr^{3+}, by nutritional effects of Cr^{3+} and the involved of Cr^{6+} in the process of carcinogenesis. Gjerde et al. [5] developed an anion-exchange method to perform chromium speciation that could be carried out under acidic pH conditions. Their aim was to have a medium in which both Cr^{3+} and Cr^{6+} were soluble. Escobar et al. [6] successfully applied their method in the determination of Cr^{3+} in water and food samples. Also, Madrakian et al. [7] established a simple, selective, and sensitive fluorescence quenching method for the determination of Cr^{6+}. In the second-part of this work, specific surface area, crystal phase, morphology, and optical properties of the prepared Cr_2O_3 nanoparticles were examined. Finally, the synthesized nanoparticles (NPs) were tested by

* Corresponding author.

Presented at the First International Congress of Energy and Industrial Process Engineering (ICEIPE'22) 23–25 May 2022, Algiers, Algeria

photostabilization of 2-aminophenol (2AP) under UV irradiation. To the best of our knowledge, this kind of study has never been reported on Cr-NPs.

2. Materials and methods

Chromium three oxide colloidal NPs were chemically synthesized from chromium six oxide, which is water soluble (0.05 M of CrO_3 in water), in the presence of $NaBH_4$ (0.125, 0.25 and 1 M) as the reducing agent, Fig. 1. We had chosen those quantities of different products by varying their molarity. All experiments were performed at room temperature and all the products were used without any further purification. In this experiment, Cr_2O_3 NPs were separated from the solution phase by ultra-centrifugation at 400 rpm for 30 min. The separated NPs were then washed with distilled water several times by re-suspension and ultra-centrifugation cycles consecutively. The collected samples were then characterized. And used for the photo-stabilisation of 2AP.

3. Results and discussion

3.1. Brunauer–Emmett–Teller analysis and UV-Visible spectroscopy

The specific surface area of the powder was measured by the Brunauer–Emmett–Teller method (BET). The BET measurement was conducted using a Quantachrome NovaWin, Quantachrome Instruments v 11.0. The values of the specific surface area of mesoporous powders changes according to the $NaBH_4$ concentration (66.06, 130 and 65.45 m^2/g), (Fig. 2a). The Cr_2O_3 nanopowders (NPWs) synthesized was type II, which is most frequently found when adsorption occurs on nonporous powders or powders with diameters exceeding micropores. The NPWs with radius between 2~50 nm were classified, by the L'IUPAC, as mesoporous NPWs and in the current work this was 3.86, 3.66 and 4.84 nm (Fig. 2b). The inflection point occurred near the completion of the first adsorbed monolayer. The type of hysteresis loop for concentrations 0.25 and 1 M of $NaBH_4$ were type 'H3' (non-rigid aggregates of plate-like particles (slit-shaped pores)) and for 0.125 M of $NaBH_4$ the type was 'H4', narrow slit pores including pores in the micropore region.

The UV-Vis spectroscopy of different oxidation states of chromium has been widely studied. Chromium was detected, by UV-Vis, due to its specific peaks [8–12]. Jin et al. [13] found the same results that were observed in the current investigation for liquid UV-Vis analysis (colloidal) (Fig. 3a). For Cr^{6+}, the peaks were at '257 and 356 nm' [13] in the current work '257 and 349 nm'. Also for Cr^{3+}, the peaks were at '273 and 375 nm' [13], in present work corresponding respectively to '0.125, 0.25 and 1 M of $NaBH_4$', for the first peak: 273, 267 and 269 nm and for the second-peak to 372, 371 and 372 nm.

The solid UV-Vis analysis (NPWs) (Fig. 3b), revealed three peaks at 268, 396 and 593 nm for the first concentration of $NaBH_4$ (0.125 M), at 268, 397 and 603 nm for the second-concentration (0.25 M) and finally for the third concentration peaks were at 268, 387 and 606 nm. These results were similar to other works [14,15]. Zavitsanos et al. [16] found two maxima in the region of 410 and 575 nm, attributed to the ($^4A_{2g}\rightarrow{}^4T_{1g}$) and the ($^4A_{2g}\rightarrow{}^4T_{2g}$) Cr^{3+} transitions, respectively. In the UV-Visible spectrum, a widening of the absorption peak, indicates the aggregation of NPs. The largest half-height width of the second-peak was the 2nd NPWs. The more the concentration of $NaBH_4$ was increased the further the first peak moved to the smaller wavelength. For the second-peak, it stayed approximately at the same position (272, 271 and 272 nm).

3.2. Scanning electron microscopy, energy-dispersive X-ray analysis and Fourier-transform infrared spectroscopy

Several studies on synthesis of chromium three oxide have been reported [17–19]. The investigators obtained NPs in the range of 50 nm–39 μm. The MEB images of the

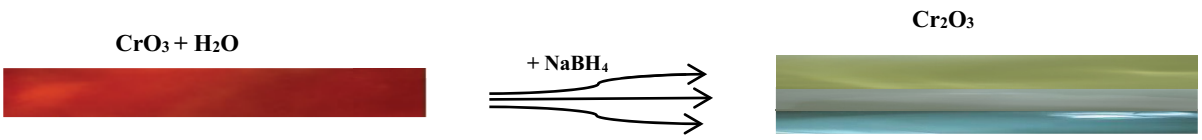

Fig. 1. Reducing process and the change of color for the different amounts of $NaBH_4$.

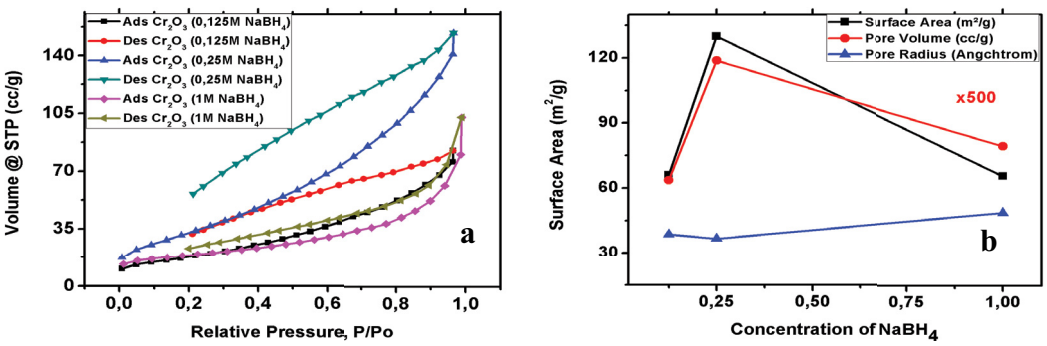

Fig. 2. (a) Nitrogen adsorption and desorption of Cr_2O_3 NPWs (for 0.125, 0.25 and 1 M of $NaBH_4$) and (b) analyzed BET results of Cr_2O_3 NPWs.

current NPWs, are shown in Fig. 4. It can be seen that the NPs were nanometrical, with sizes between 22–150 nm for the first sample, between 17–68 nm for the second-sample and for the third one, sizes between 19–80 nm (determined by ImageJ). This means that the second-quantity of $NaBH_4$ is the one that gives the smallest NPs sizes, the images also showed an even size distribution.

Scientists use energy-dispersive X-ray analysis (EDX or EDS) to determine which species are present in each sample. The present investigation employed a 'Zeiss Smart EDX' an EDX analysis, used together with a 'Zeiss' scanning electron microscope (SEM). The EDX (Fig. 5) shows that all samples contained chromium and oxygen. Jin et al. [13] reported an EDX pattern which was similar to the current results. Oxygen and chromium were the highest percent by mass in the first sample (0.125 M $NaBH_4$), 57.30 (3.62% of error) and 35.04% (2.07% of error), respectively. The second-sample contained more 'Cr' and less of 'O', but there was some 'Na' (the mass was 7.07% with a 12.42% of error). This was due to the high concentration of $NaBH_4$ (0.25 M of $NaBH_4$), 47.33 (5.15% of error) of oxygen and 39.93% (2.21% of error) for chromium. Finally, with the 1 M of $NaBH_4$, the ratio was 45.04 (5.76% of error) of oxygen and 25.30% (2.24% of error) for chromium and for 'Na', the mass was 22.42% with a 9.06% of error.

The Fourier-transform infrared spectroscopy (FT-IR) of different Cr-NPWs, are shown in Fig. 6. The broad bands appearing around 3,433 and 3,169 cm^{-1} were attributed to the stretching vibrations of hydrogen-bonded water molecules and hydroxyl groups, and the absorption of H_2O by the sample from atmospheric moisture [20]. Kamble et al. [21] mentioned that metal oxide showed absorption bands below 1,000 cm^{-1} due to inter-atomic vibrations. The band at 1,630 cm^{-1} exhibited the bending OH-group. The current study found a lot of similarities with the work of Vuurman et al. [22]. The latter attributed the region between

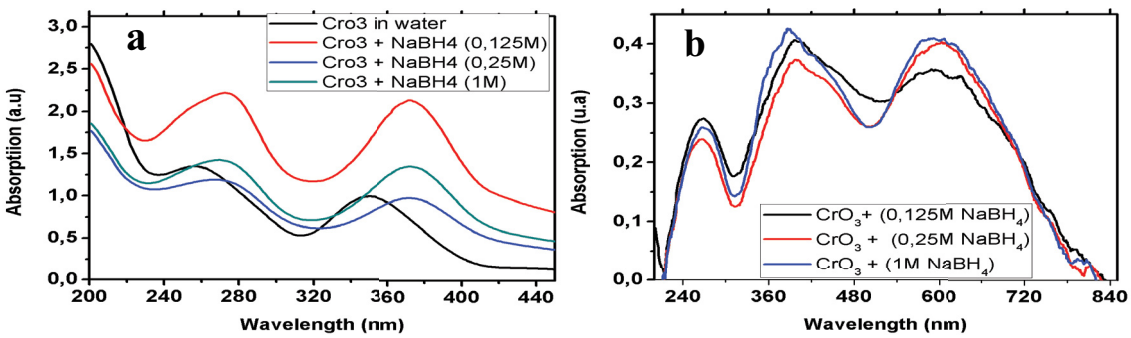

Fig. 3. UV-Visible patterns of (a) colloidal chromium and (b) Cr_2O_3 NPWs.

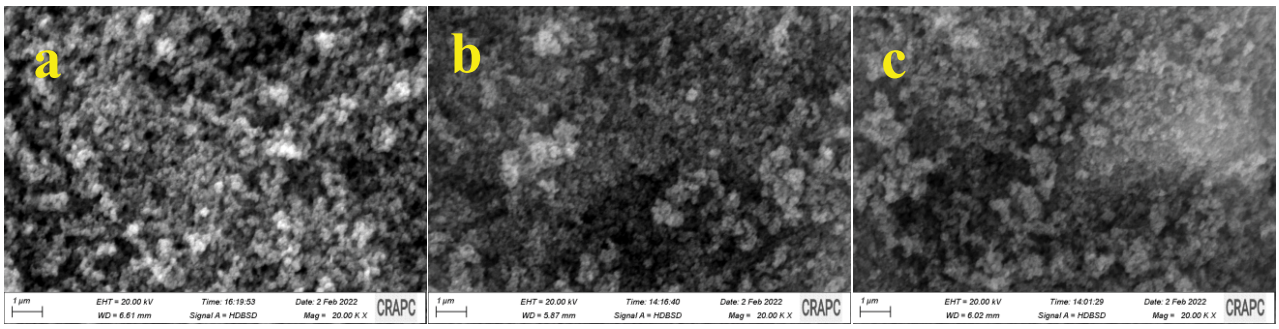

Fig. 4. MEB pictures of chromium NPs (0.125, 0.25 and 1 M of $NaBH_4$, respectively, a, b and c).

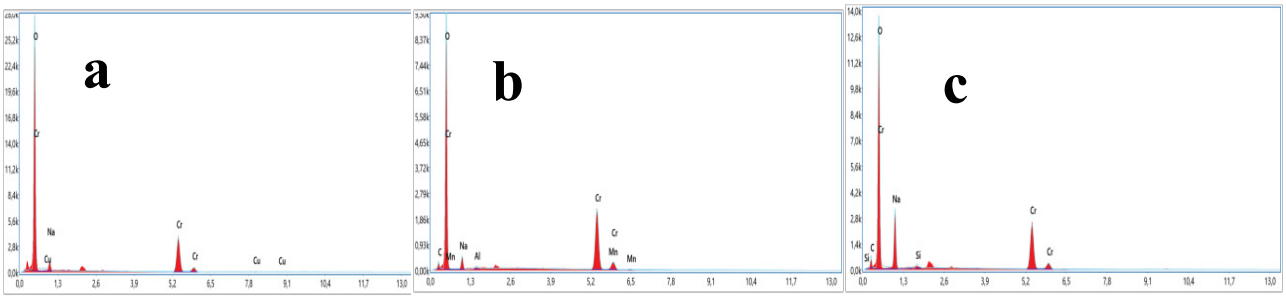

Fig. 5. EDX spectroscopy of chromium NPs (0.125, 0.25 and 1 M of $NaBH_4$, respectively, a, b and c).

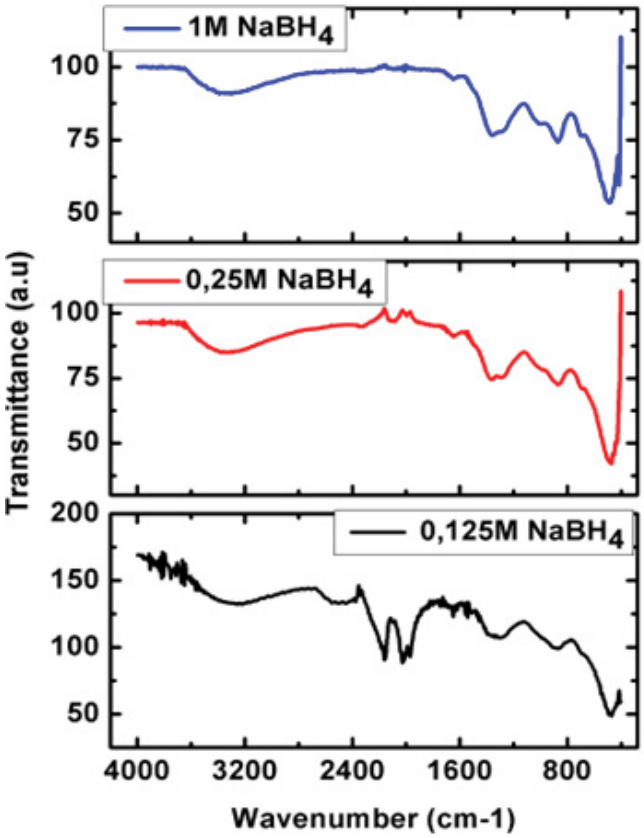

Fig. 6. FT-IR pattern of chromium-NPWs.

2,150–1,850 cm^{-1} to infrared (IR) absorptions in the chromium oxygen overtone stretching, two bands at 2,010 and 1,986 cm^{-1} in the first Cr=O overtone region, and two bands at around 1,020 and 1,005 cm^{-1} in the Cr=O stretching region. They also reported that the presence of two bands in the overtone region supported the presence of two surface Cr=O species, which meant that two kinds of Cr=O bands were present in the molecule. Vuurman et al. [22] mentioned that the broadness of the 880–850 cm^{-1} bands in all the spectra indicated a wide range of OCrO bond distances. Rakesh et al. [23], said that the bands at 967–1,037 cm^{-1} were assigned to Cr=O vibrations, 585–641 cm^{-1} was assigned to Cr–O vibrations and 1,046–1,085 cm^{-1} were assigned to Cr–O–Cr vibrations. The bands between 401 and 447 cm^{-1} were attributed to ν(Cr–O) [24]. The 'Cr–O' band was between 413 and 442 cm^{-1} [25,26]. Sousa et al. [27], reported that the IR peak at 401 cm^{-1} was an indication of crystalline Cr_2O_3. Harrison et al. [28], noted that the antisymmetric CrOCr stretch had an energy of 870 cm^{-1}.

3.3. Application

The ability of 2AP to oxidise very quickly gives it multiple applications, for example as photographic developers and catalytic properties of NPs. This application is directly related to the dye industry [29] and to the environmental impact, due to the biocompatibility of Cr_2O_3 [30], compared to CrO_3, which is harmful to living tissue [31]. One of the nanopowders (NPWs) was used to assess the behavior of 2AP during exposure to UV light (210 nm). The chosen chromium NPW, was the one with the highest specific area (0.25 of $NaBH_4$, 130 m^2/g). The impact on the stabilization of 2AP as a function of time was monitored. Fathalla et al. [32] used 2AP as a substrate for their work. They evaluated the catalytic performance of their compounds (four different products) for the oxidative coupling of 2AP to 2-aminophenoxazin-3-one (APO), by UV-Vis measurement. They followed the growth of APO (a peak at 431 nm as in the current work) in an aqueous solution of 2AP (a peak at 280 nm, same as in the present work). The study by Elder [33] revealed that 2AP is safe as a cosmetic ingredient. They reported that chlorination of drinking water may increase the toxicity of 2AP. The main use of 2AP is as a powerful reduction agent as a synthetic precursor. Its products are represented in virtually all classes of dyes [29]. The proximity of the amino and hydroxyl groups on the benzene ring of 2AP and the ease of condensation with appropriate reagents, makes 2AP an excellent intermediate in the synthesis of heterocyclic systems [34]. This product has been used as an inhibitor of inflammation [34].

The 2AP is water soluble. A solution with a low concentration of 2AP was prepared by dissolving in distilled water. The exposure to UV irradiation was made in a controlled temperature bath to simulate the heat of the sun, with magnetic agitation. The measurements were made by UV-Vis spectroscopy, every 1 h or a 1/2 h, to see the changes in our solution composition (rising or decreasing of peaks), in both cases(with or without NPW).

Referred to the previous works [35,36], the peak at 250–300 nm was attributed to 2AP and the one situated at 350–500 nm was attributed to APO. The current samples, were monitored with and without adding 0.02 g of NPW to 100 mL of 2AP solution. The mixture was placed in ultrasound for 30 min. After that the mixture was exposed to the UV irradiation. The 2AP was irradiated with UV irradiation for 6 h, in the absence of our NPW (Fig. 7a). It can be seen that with every 1 h of irradiation, the peak of 2AP (250–300 nm) decreased. In the other side, the peak of APO, gain of intensity was observed every 1 h compared to the peak of 2AP. The addition of Cr-NPW had a stabilizing effect (Fig. 7b). For the chosen NPW, very high stability was observed compared with the solution of 2AP alone. The stability and the inhibition power is shown in Fig. 7c and d, respectively for the first and the second-peak. It can be seen that the presence of the Cr-NPW, has a height efficiency to stabilize 2AP and prevent the formation of APO, due to the small variation of the concentration of both products with and without Cr-NPW.

4. Conclusions

The current investigation has succeeded in the synthesis of NPWs (SEM imaging) of chromium three oxide, the composition is proved by EDX analysis and FT-IR, the samples are colloids and powders with green colour. It can be seen the characteristic peaks in the UV-Vis spectroscopy of Cr^{3+}, which indicate also the formation of the desired metal oxide. These powders are mesoporous (BET measurements). The Cr-NPW was found to be effective in the photo-stabilization of 2AP from oxidation to APO (UV-Vis spectroscopy).

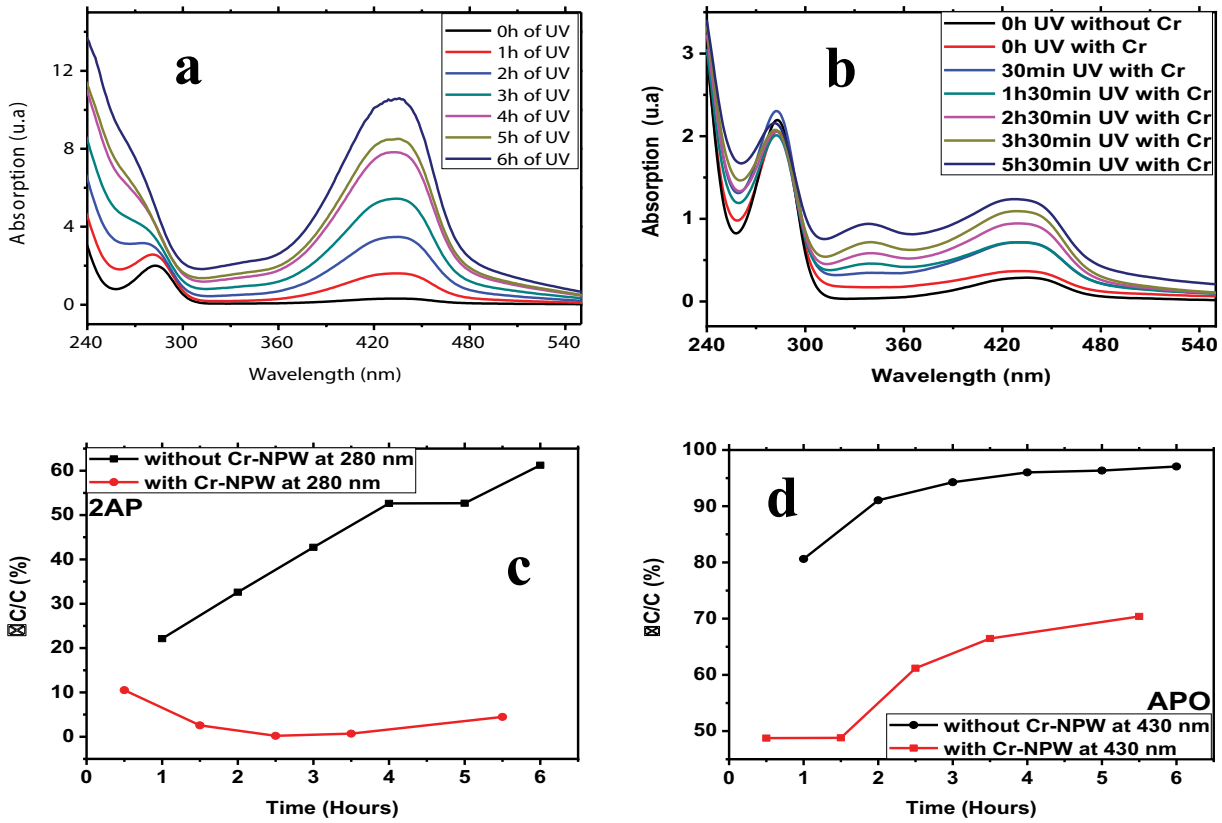

Fig. 7. (a) 2AP irradiated with UV irradiation (210 nm) for 6 h without the presence of Cr-NPWs. (b) 2AP irradiated with UV irradiation (210 nm) for 5 h and 30 min in the presence of Cr-NPW (0.25 M of $NaBH_4$), (c and d) the stability of 2AP and APO with and without Cr-NPW.

This was due to the high efficiency of Cr-NPW in protecting and stabilizing 2AP from oxidation to APO under UV irradiation. It was noticed that UV-light accelerated the formation of APO when the 2AP was by itself compared to when it was in the dark or under visible light.

References

[1] T. Madrakian, A. Afkhami, M. Mohammadnejad, Application of organized media for rapid spectrofluorimetric determination of trace amounts of Cr(VI) in the presence of Cr(III), Bull. Korean Chem. Soc., 30 (2009) 1252–1256.

[2] M.K. Jamali, T.G. Kazi, M.B. Arain, H.I. Afridi, N. Jalbani, A.R. Memon, Heavy metal contents of vegetables grown in soil, irrigated with mixtures of wastewater and sewage sludge in Pakistan, using ultrasonic-assisted pseudo-digestion, J. Agron. Crop Sci., 193 (2007) 218–228.

[3] M. Pouzar, M. Průšová, P. Prokopčáková, T. Černohorský, J. Wiener, A. Krejčová, LIBS analysis of chromium in samples of dyed wool fabric, J. Anal. At. Spectrom., 24 (2009) 685–688.

[4] K. Salnikow, A. Zhitkovich, Genetic and epigenetic mechanisms in metal carcinogenesis and cocarcinogenesis: nickel, arsenic and chromium, Chem. Res. Toxicol., 21 (2008) 28–44.

[5] D.T. Gjerde, D.R. Wiederin, F.G. Smith, B.M. Mattson, Metal speciation by means of microbore columns with direct-injection nebulization by inductively coupled plasma atomic emission spectroscopy, J. Chromatogr. A, 640 (1993) 73–78.

[6] R. Escobar, Q. Lin, A. Guiraúm, F.F. de la Rosa, Flow injection chemiluminescence method for the selective determination of chromium(III), Analyst, 118 (1993) 643–647.

[7] T. Madrakian, A.H. Mohammadzadeh, S. Maleki, A. Afkhami, Preparation of polyacrylonitrile nanofibers decorated by N-doped carbon quantum dots: application as a fluorescence probe for determination of Cr(VI), New J. Chem., 42 (2018) 18765–18772.

[8] W. Ahmad, A.S. Bashammakh, A.A. Al-Sibaai, H. Alwael, M.S. El-Shahawi, Trace determination of Cr^{3+} and Cr^{6+} species in water samples via disp. liquid–liquid microextraction and microvolume UV–Vis spectr. therm., speciation study, J. Mol. Liq., 224 (2016) 1242–1248.

[9] Z. Zhang, D. Liba, L. Alvarado, A. Chen, Separation and recovery of Cr(III) and Cr(VI) using electrodeionization as an efficient approach, Sep. Purif. Technol., 137 (2014) 86–93.

[10] L. Leita, A. Margon, A. Pastrello, I. Arčon, M. Contin, D. Mosetti, Soil humic acids may favour the persistence of hexavalent chromium in soil, Environ. Pollut., 157 (2009) 1862–1866.

[11] L. Xia, E. Akiyama, G. Frankel, R. McCreery, Storage and release of soluble hexavalent chromium from chromate conversion coatings equilibrium aspects of Cr^{VI} concentration, J. Electrochem. Soc., 147 (2000) 2556, doi: 10.1149/1.1393568.

[12] K. Chen, L. Bocknek, B. Manning, Oxidation of Cr(III) to Cr(VI) and production of Mn(II) by synthetic manganese(IV) oxide, Crystals, 11 (2021) 443, doi: 10.3390/cryst11040443.

[13] R. Jin, Y. Liu, G. Liu, T. Tian, S. Qiao, J. Zhou, Characterization of product and potential mechanism of Cr(VI) reduction by anaerobic activated sludge in a sequencing batch reactor, Sci. Rep., 7 (2017) 1681, doi: 10.1038/s41598-017-01885-z.

[14] A.A. Wesam, B.T. Chiad, A.J.H. Al-Wattar, Q.M. Salman, Spectroscopic comparison of UV-VIS electronic transitions of Cr ions in solution, sol and Xerogel silica matrices, Nano Sci. Nano Technol.: An Indian J., 6 (2012) 90–96.

[15] Z.H. Yahia, H.N. Bayakly, M. Shafi, S. Painter, V. Taylor, J. Greene, K. Rosli, Interaction of malate and lactate with chromium(III) and iron(III) in aqueous solutions, Synth. React. Inorg. Metal-Org. Nano-Metal Chem., 7 (2005) 515–522.

[16] K. Zavitsanos, K. Tampouris, A.L. Petrou, Reaction of chromium(III) with 3,4-dihydroxybenzoic acid: kinetics and

mechanism in weak acidic aqueous solutions, Bioinorg. Chem. Appl., 2008 (2008) 212461, doi: 10.1155/2008/212461.
[17] Z. Pei, J. Pei, H. Chen, L. Gao, S. Zhou, Hydrothermal synthesis of large sized Cr_2O_3 polyhedrons under free surfactant, Mater. Lett., 159 (2015) 357–361.
[18] S. Tian, X. Ye, Y. Dong, W. Li, B. Zhang, B. Li, H. Feng, Production and characterization of chromium oxide (Cr_2O_3) via a facile combination of electrooxidation and calcination, Int. J. Electrochem. Sci., 14 (2019) 8805–8818.
[19] S. Khamlich, E. Manikandan, B.D. Ngom, J. Sithole, O. Nemraoui, I. Zorkani, R. McCrindle, N. Cingo, M. Maaza,. Synthesis, characterization, and growth mechanism of α-Cr_2O_3 monodispersed particles, J. Phys. Chem. Solids, 72 (2011) 714–718.
[20] S.M. Abo-Naf, M.S. El-Amiry, A.A. Abdel-Khalek, FT-IR and UV–Vis optical absorption spectra of γ-irradiated calcium phosphate glasses doped with Cr_2O_3, V_2O_5 and Fe_2O_3, Opt. Mater., 30 (2008) 900–909.
[21] B.B. Kamble, M. Naikwade, K.M. Garadkar, R.B. Mane, K.K.K. Sharma, B.D. Ajalkar, S.N. Tayade, Ionic liquid assisted synthesis of chromium oxide (Cr_2O_3) nanoparticles and their application in glucose sensing, J. Mater. Sci.: Mater. Electron., 30 (2019) 13984–13993.
[22] M.A. Vuurman, I.E. Wachs, D.J. Stufkens, A. Oskam, Characterization of chromium oxide supported on Al_2O_3, ZrO_2, TiO_2, and SiO_2 under dehydrated conditions, J. Mol. Catal., 80 (1993) 209–227.
[23] Rakesh, S. Ananda, N.M. Made Gowda, Synthesis of chromium(III) oxide nanoparticles by electrochemical method and Mukia Maderaspatana plant extract, characterization, $KMnO_4$ decomposition and antibacterial study, Mod. Res. Catal., 2 (2013) 127–135.
[24] K.S. Budiasih, C. Anwar, S.J. Santosa, H. Ismail, Preparation and Infrared Spectroscopic Studies of Chromium(III) – Glutamic Acid Complexes, Antidiabetic Supplement Candidates, Proc. Int. Conf. Indonesian Chem. Soc., Malang, Indonesia, 2012.
[25] K.S. Budiasih, C. Anwar, S.J. Santosa, H. Ismail, Synthesis and characterization of chromium(III) complexes with L-glutamic acid, glycine and L-cysteine, Int. J. Biotechnol. Bioeng., 7 (2013) 458–462.
[26] T. Ivanova1, K. Gesheva, A. Cziraki, A. Szekeres, E. Vlaikova, Structural transformations and their relation to the optoelectronic properties of chromium oxide thin films, J. Phys.: Conf. Ser., Fifteenth International Summer School on Vacuum, Electron and Ion Technologies (VEIT 2007) 17–21 September 2007, Bulbank Hotel, Sozopol, Bulgaria, 113 (2008) 012030, doi: 10.1088/1742-6596/113/1/012030.
[27] P.M. Sousa, A.J. Silvestre, N. Popovici, M.L. Paramês, O. Conde, KrF Laser CVD of Chromium Oxide by Photodissociation of $Cr(CO)_6$, Mater. Sci. Forum, 455–456 (2004) 20–24.
[28] G.H. Philip, D. Wayne, Catalytic activity, surface redox properties, and structural evolution during the thermal processing of chromium-promoted ceria oxidation catalysts, Chem. Mater., 13 (2001) 1708–1719.
[29] S. Mitchell, R. Waring, Aminophenols, Kirk-Othmer Encyclopedia of Chemical Technology, 2000, doi: 10.1002/0471238961.0113091413092003.a01.
[30] S.A. Khan, S. Shahid, S. Hanif, H.S. Almoallim, S.A. Alharbi, H. Sellami, Green synthesis of chromium oxide nanoparticles for antibacterial, antioxidant anticancer, and biocompatibility activities, Int. J. Mol. Sci., 22 (2021) 502, doi: 10.3390/ijms22020502.
[31] T. Dahryn, T. Mahendra, B. Alice, N. Gopal, J. Snehasis, Impact of consciousness energy healing treatment on the physicochemical and thermal properties of chromium trioxide (CrO_3), Pharm. Sci. Anal. Res. J., 2 (2019) 180016.
[32] K.S. Fathalla, H.A. El-Ghamry, M. Gaber, Ru(III) complexes of triazole based Schiff base and azo dye ligands: an insight into the molecular structure and catalytic role in oxidative dimerization of 2-aminophenol, Inorg. Chem. Commun., 129 (2021) 108616, doi: 10.1016/j.inoche.2021.108616.
[33] R. Elder, Final report on the safety assessment of *p*-aminophenol, *m*-aminophenol and *o*-aminophenol, Int. J. Toxicol., 7 (1988) 279–333.
[34] M. Terashima, A facile synthesis of 2-substituted benzoxazoles, Synthesis, 6 (1982) 484–485.
[35] O.A. Mehrez, F. Dossier-Berne, B. Legube, Oxidation of 2-aminophenol to 2-amino-3H-phenoxazin-3-one with monochloramine in aqueous environment: a new method for APO synthesis?, Chemosphere, 145 (2016) 464–469.
[36] A. Sahoo, S. Kumar, N. Dehury, S. Patra, A porous trimetallic Au@Pd@Ru nanoparticle system: synthesis, characterisation and efficient dye degradation and removal, J. Mater. Chem. A, 38 (2015) 19376–19383.